

Freezing and melting criteria in non-equilibrium

This article has been downloaded from IOPscience. Please scroll down to see the full text article.

2001 J. Phys.: Condens. Matter 13 9197

(<http://iopscience.iop.org/0953-8984/13/41/311>)

View [the table of contents for this issue](#), or go to the [journal homepage](#) for more

Download details:

IP Address: 171.66.16.226

The article was downloaded on 16/05/2010 at 14:58

Please note that [terms and conditions apply](#).

Freezing and melting criteria in non-equilibrium

G P Hoffmann and H Löwen

Institut für Theoretische Physik II, Heinrich-Heine-Universität Düsseldorf, Universitätsstraße 1,
D-40225 Düsseldorf, Germany

Received 3 August 2001, in final form 28 August 2001

Published 28 September 2001

Online at stacks.iop.org/JPhysCM/13/9197

Abstract

Using non-equilibrium computer simulations, it is shown that various phenomenological criteria for melting and freezing hold not only in equilibrium but in steady-state non-equilibrium as well. In particular, we study the steady state of charge-polydisperse Brownian particles shaken by a time-dependent oscillatory electric field. Among these criteria are the Lindemann melting rule, the Hansen–Verlet freezing rule and the dynamical freezing criterion proposed for colloidal fluids by Löwen, Palberg and Simon.

1. Introduction

The freezing and melting transition is far from being understood from first principles, even in thermodynamic equilibrium and for relatively simple systems interacting via a radially symmetric pair potential [1]. The essential difficulty arises from the collective many-body effects resulting in a broken translational symmetry across freezing. Recent microscopic descriptions [2, 3] are based either on the liquid phase (such as density functional approaches) or on the crystal phase (such as solid–defect theories) but it is fair to say that a *fully predictive theory* with the interactions between the particles as the only input is not available. Therefore *phenomenological criteria* based on empirical observations in experiments or computer simulations have been very important for estimating the location of the freezing and melting lines. In general, these criteria work if the freezing occurs at high densities, in which case the relative density jump across freezing is small. The most traditional criterion is the *Lindemann melting rule* [4]: it states that a solid melts if the root mean square displacement of particles around their ideal lattice positions is roughly ten per cent of their nearest-neighbour distance. This rule has been tested for different materials [5, 6] and model fluids [7, 8] and indeed the relative displacement L was found to be within five to twenty per cent at melting. The Lindemann criterion cannot be used to describe two-dimensional melting because the root mean square displacement diverges there [9]. It can, however, be generalized by considering relative displacements between neighbouring particles only [10]. Furthermore the Lindemann rule was found recently to be valid in higher spatial dimensions [11], for re-entrant melting [12] and for interfacial freezing transitions [13].

A second criterion is the *Hansen–Verlet freezing rule* [14]. It states that a (three-dimensional) liquid freezes if the amplitude S_m of the first maximum in the structure factor $S(k)$ exceeds 2.85. For two-dimensional freezing, however, the actual value of the amplitude is getting much larger at freezing and is about 5.5 [15].

Third, a *dynamical freezing rule* for Brownian colloidal fluids was proposed by Löwen, Palberg and Simon (LPS) [8]. This criterion is based on the ratio D_L/D_0 between the short-time and long-time diffusion coefficients. A fluid freezes if this ratio becomes smaller than ten per cent. This criterion was shown to be also valid in two dimensions [16] and was recently related to the Hansen–Verlet freezing rule via mode-coupling theory [17, 18]. It is particularly useful for the crystallization transition of colloidal suspensions [19].

All these criteria have been developed and applied so far in equilibrium. In this paper we investigate whether these criteria are also valid in non-equilibrium situations [20]. Freezing and melting in non-equilibrium is, of course, much more complicated, as the traditional thermo-statistical concepts break down. In many non-equilibrium cases, however, the systems run into a steady-state situation where structural and dynamical correlations as well as phase transitions can be defined [21–24]. Consequently, the Lindemann parameter L , the liquid structure factor $S(k)$ and the diffusion coefficients are still well-defined quantities there. Therefore it is tempting to check whether the phenomenological criteria are fulfilled in non-equilibrium. In fact, in experiments on two-dimensional colloids by Grier and Murray [25], the LPS criterion for freezing was used in non-equilibrium and was confirmed there.

In this work we consider a particular steady-state non-equilibrium situation: a slightly polydisperse Brownian Yukawa fluid is driven by a space-independent but time-dependent oscillatory external field that couples differently to the different particles according to their polydispersity. We have shown recently [26] that such a field shifts the freezing transition with respect to equilibrium freezing. The shift depends strongly on the field amplitude, scaling with the square of the relative polydispersity, and vanishes for very large field frequencies. In this paper we use extensive computer simulations to test the validity of the three different freezing and melting criteria mentioned above. We find that all three rules are indeed fulfilled provided the polydispersity is not too large which means that the system is rather close to equilibrium (see our discussion in section 3). Our results suggest that the freezing criteria are robust when turning from equilibrium to non-equilibrium systems, provided the system is not too far away from equilibrium. Thus our findings will be helpful in interpreting experiments which are typically carried out in non-equilibrium [25]. As a by-product, we also confirm that the freezing criteria are valid in equilibrium for small charge polydispersities. In this case, similar tests for the Hansen–Verlet rule and the Lindemann criterion have already been made by Tata and Arora [27, 28].

The paper is organized as follow. In section 2, we define our model. In section 3 we describe our simulation method. The different freezing criteria are tested and further results for the inherent system anisotropy are presented in section 4. We conclude in section 5.

2. Model

Our model for non-equilibrium Brownian dynamics of charge-polydisperse colloids is defined as follows [26]: N colloidal particles confined to a volume Ω (with a fixed number density $\rho = N/\Omega$ defining a mean interparticle spacing of $a = \rho^{-1/3}$) are held at fixed temperature T . Two colloidal particles i and j are interacting via an effective screened Coulomb pair potential [29, 30]

$$V_{ij}(r) = Z_i Z_j U_0 \sigma \frac{\exp(-\lambda(r - \sigma)/\sigma)}{r} \quad (1)$$

where r is the interparticle distance, U_0 sets an energy and σ a length scale. The quantity λ is a dimensionless screening parameter. $Z_i > 0$ denotes the reduced colloidal charge of the i th colloidal particle. The charges Z_i are drawn from a given distribution $p(Z)$ around a mean value \bar{Z} which can be set equal to unity without loss of generality. The width of the distribution is governed by the prescribed relative polydispersity

$$p_Z = \sqrt{Z^2 - 1}.$$

In our simulations we took either a bimodal distribution

$$p(Z) = [\delta(Z - 1 + p_Z) + \delta(Z - 1 - p_Z)]/2 \quad (2)$$

or a rectangular distribution

$$p(Z) = \begin{cases} 1/(\sqrt{12}p_Z) & \text{for } |Z - 1| < \sqrt{3}p_Z \\ 0 & \text{otherwise.} \end{cases} \quad (3)$$

Apart from the direct interaction (1), there is an external oscillatory force $\vec{F}_i(t)$ resulting from an ac electric field which acts on the i th colloidal particle in the z -direction:

$$\vec{F}_i(t) = \vec{e}_z Z_i E_0 \sin(\omega t) \quad (4)$$

where ω is the field frequency, E_0 the field amplitude and \vec{e}_z the unit vector along the z -direction. Neglecting hydrodynamic interactions, the stochastic Langevin equations for the colloidal trajectories $\vec{r}_i(t) = (x_i(t), y_i(t), z_i(t))$ ($i = 1, \dots, N$) read as

$$\frac{k_B T}{D_0} \frac{d\vec{r}_i}{dt} = -\vec{\nabla}_{\vec{r}_i} \sum_{j \neq i} V_{ij}(|\vec{r}_i - \vec{r}_j|) + \vec{F}_i(t) + \vec{F}_i^{(R)}(t) \quad (5)$$

where $k_B T$ is the thermal energy, D_0 is the short-time diffusion coefficient and the random forces $\vec{F}_i^{(R)}$ describe the kicks of the solvent molecules acting on the i th colloidal particle. These random forces are Gaussian random numbers with zero mean:

$$\overline{\vec{F}_i^{(R)}} = 0$$

and variance

$$\overline{(\vec{F}_i^{(R)})_\alpha(t) (\vec{F}_j^{(R)})_\beta(t')} = \frac{2(k_B T)^2}{D_0} \delta_{\alpha\beta} \delta_{ij} \delta(t - t') \quad (6)$$

guaranteeing that

$$D_0 = \lim_{t \rightarrow 0} \overline{(\vec{r}_i(t) - \vec{r}_i(0))^2 / 6t}. \quad (7)$$

The subscripts α and β stand for the three Cartesian components. As has been shown earlier, the external field has no influence for a monodisperse system apart from adding a trivial overall dynamical mode [26]. Hence a finite polydispersity $p_Z > 0$ is essential to drive the system into real non-equilibrium and the polydispersity itself measures the ‘distance’ from equilibrium.

3. Simulation methods and diagnostics for the freezing and melting transition

We solved the Langevin equations (5) by means of a finite-time step Brownian dynamics simulation [31] using $N = 864$ particles in a cubic box with periodic boundary conditions. The Brownian timescale is set by $\tau = k_B T a^2 / U_0 D_0$ and a typical size of the time step was $\Delta t = 0.003\tau$. The system was carefully ‘equilibrated’ for a time of typically 100τ until a steady state was reached. In order to reduce the multi-dimensional parameter space we kept the density, the field amplitude and the dimensionless screening parameter fixed to $\rho = 1/\sigma^3$,

$E_0 = 10.5U_0/a$, $\lambda = 5.8$, such that the crystalline structure is either face-centred cubic (fcc) or hexagonal close packed (hcp) with random occupancy for small p_Z . We studied the system as a function of reduced temperature $T^* = k_B T/U_0$, starting with small (large) temperatures and continuing our simulations by gently heating (cooling) the system, and further varied the polydispersity and the field frequency. The parameter combinations investigated are summarized in table 1. Note that $\omega = 0$ implies a vanishing field and thus an equilibrium situation.

Table 1. Phase transition temperature T_0^* , Lindemann parameter L , amplitude S_m of the first maximum in the liquid structure factor and the ratio of long-time and short-time self-diffusion coefficients, D_L/D_0 , at freezing/melting for different parameter combinations characterized by the polydispersity p_Z and field frequency $\omega\tau$. Note that $\omega\tau = 0$ implies an equilibrium situation. If the given polydispersity is marked by a star, the system was bimodal; otherwise the polydispersity was drawn from a rectangular distribution. The number in brackets indicates the error of the last digit.

p_Z	$\omega\tau$	T_0^*	L	S_m	D_L/D_0
0	0	0.204(14)	0.183(7)	2.9(2)	0.10(2)
0.05	0	0.20(2)	0.183(7)	2.9(2)	0.10(2)
0.05	1.57	0.19(1)	0.186(7)	3.1(3)	0.11(2)
0.05(*)	0	0.205(15)	0.184(7)	2.9(2)	0.10(2)
0.05(*)	6.28	0.205(15)	0.187(9)	2.9(2)	0.10(2)
0.15(*)	0	0.180(9)	0.190(9)	3.0(2)	0.10(2)
0.15(*)	6.28	0.178(13)	0.181(9)	3.0(3)	0.11(2)

In particular, we are interested in the freezing/melting transition in the non-equilibrium steady state. We detect this transition by means of an analysis of the temperature dependence of the Lindemann parameter L in the crystalline state, defined through

$$L = \sqrt{\left\langle \sum_{i=1}^N (\vec{r}_i(t) - \langle \vec{r}_i(t) \rangle)^2 \right\rangle} / a. \quad (8)$$

Here the mean interparticle spacing a is close to the solid lattice constant. The brackets $\langle \dots \rangle$ denote an ensemble, a polydispersity and a time average in the steady state at discrete times nt_p set by the period $t_p = 2\pi/\omega$ of the electric field. Neglecting hopping processes in the solid, the quantity $\langle (\vec{r}_i(t) - \langle \vec{r}_i(t) \rangle)^2 \rangle$ becomes time independent in the solid for large times where $\langle \vec{r}_i(t) \rangle$ sets the ideal lattice positions. At this stage we remark that the square involved in the definition (8) is inherently anisotropic, but it will be shown later that the anisotropy is small.

In principle, the freezing and melting temperatures should coincide. In practice, however, there is a hysteresis loop upon heating and re-cooling the system, whose finite width indicates that the non-equilibrium freezing transition is first order. The width of the hysteresis loop can be used to estimate the error in locating the phase transition temperature. In detail, we used the following procedure. We monitored L as a function of reduced temperature T^* during the process of heating a solid; see figure 1. L increases slowly with increasing T^* . Upon reaching a characteristic temperature T_m^* , L exhibits a kink and increases much faster upon heating the system further. T_m^* is an estimate of the *melting temperature* of the solid (at least it should be an upper bound for the melting temperature). Upon further heating, L grows dramatically, indicating that a fluid phase has been reached. Thereafter the system is cooled down, resulting in a hysteresis loop for L (see figure 1) until L has practically reached the value corresponding to the original solid. The temperature T_f^* where this happens is an estimate for the *freezing*

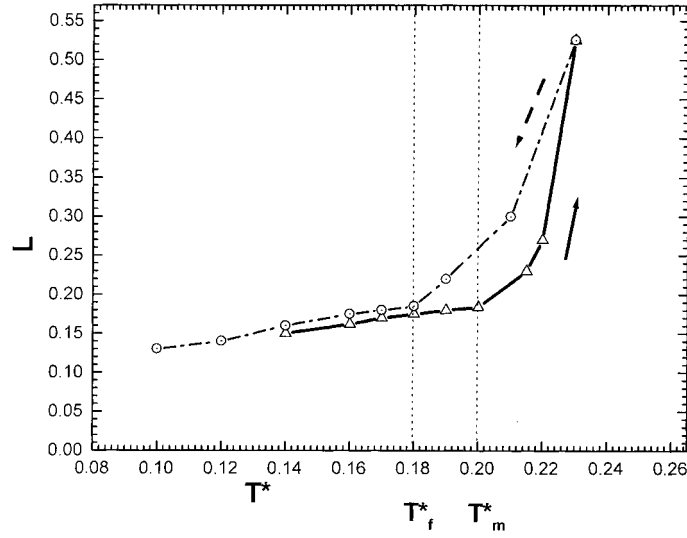


Figure 1. Lindemann parameter L versus reduced temperature T^* upon heating and subsequent cooling as indicated by the arrows. The parameters are $p_Z = 0.05$ and $\omega\tau = 1.57$. The estimates of the reduced freezing and melting temperatures T_f^* and T_m^* are indicated by the vertical dashed lines.

temperature of the fluid (at least it should be a lower bound for the freezing temperature). Hence the real phase transition temperature T_0^* should fulfil $T_f^* < T_0^* < T_m^*$. Hence it is a reasonable estimate to assume

$$T_0^* = \frac{1}{2}(T_f^* + T_m^*) \pm \frac{1}{2}(T_m^* - T_f^*). \quad (9)$$

Indeed, comparing the result obtained from our procedure with the equilibrium freezing/melting temperature of Yukawa systems as obtained by the much more accurate method of thermodynamic integration, we obtain good agreement: the parameters in the first row in table 1 lead to an exact transition temperature of $T_0^* = 0.205$ as obtained by the thermodynamic integration method [7] which agrees well with our estimate $T_0^* = 0.204 \pm 0.014$. The important fact, however, is that our method can be applied also to non-equilibrium phase transitions where the concept of thermodynamic integration breaks down.

We have further monitored the behaviour of bond-orientational order parameters Q_4 and Q_6 [32, 33] which provide a sensitive diagnostics for crystallization into fcc and hcp lattices. For example, in a fluid, Q_6 is very small while it has a value of 0.57 for an ideal fcc solid. The advantage of bond orientations is that they discriminate clearly between a crystal and an amorphous glass. Corresponding data for Q_6 within a hysteresis loop are presented in figure 2. The kink at $T^* = T_m^*$ is much less pronounced than in the Lindemann parameter development (figure 1). On the other hand, the transition back to the crystalline state during cooling is clearly seen. The fact that Q_6 goes almost back to its original value close to 0.57 (which is for an ideal fcc solid) clearly indicates that the system has refrozen into an fcc crystal.

4. Results

Using the diagnostics of the previous section [34], we determined the freezing/melting transition temperature T_0^* for seven different parameter combinations summarized in table 1. T_0^* decreases with increasing polydispersity p_Z and increasing ω , consistently with our earlier

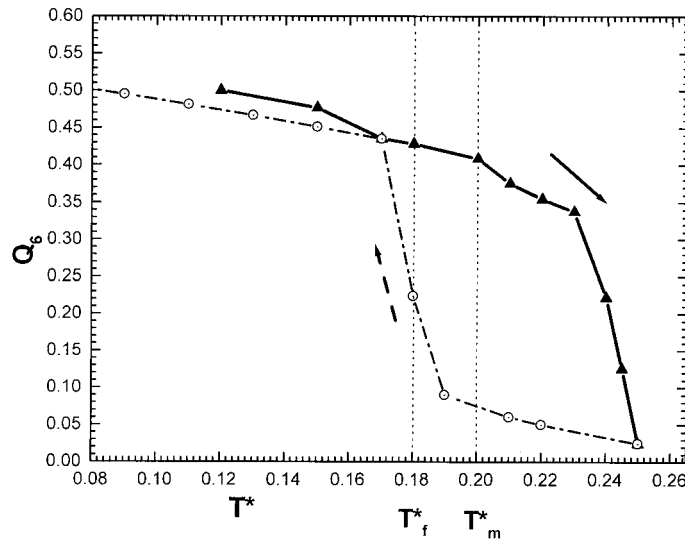


Figure 2. As figure 1, but now for the bond-orientational order parameter Q_6 .

findings [26]. For a rectangular charge distribution (3) the stable crystal exhibited an fcc structure, while we found a random occupied hcp crystal as the stable phase for the bimodal distribution (2). Once the phase transition temperature T_0^* is known, one can calculate L , S_m , D_L/D_0 at the transition in the solid and fluid phases, in order to test the freezing and melting criteria.

- (i) The first quantity is the Lindemann parameter L as defined in equation (8). Fortunately, in the crystalline state, L varies only slowly with temperature such that the value of L at the kink near T_m^* is close to L at melting; see the small error bar in table 1.
- (ii) In the fluid state near the transition, we furthermore calculated the height S_m of the first maximum in the orientationally averaged particle–particle liquid structure factor $S(k)$, defined through

$$S(k) = \frac{1}{4\pi} \int_0^{2\pi} d\phi \int_0^\pi d\theta \left\langle \frac{1}{N} \sum_{i,j=1}^N \exp[-i\vec{k} \cdot (\vec{r}_i - \vec{r}_j)] \right\rangle \quad (10)$$

where $\vec{k} = (k \cos \phi \sin \theta, k \sin \phi \sin \theta, k \cos \theta)$. In the case of a binary mixture, $S(k)$ is the number–number structure factor which is a linear superposition of the partial structure factors. The amplitude S_m of the first peak in $S(k)$ is shown in figure 3 for a cooling cycle of the fluid. S_m depends sensitively on temperature. The error (9) associated with the determination of the phase transition temperature (see equation (9)) therefore produces a large error in S_m , which is indicated in table 1 and can also be read off from figure 3 together with our estimate (9) of the phase transition temperature.

- (iii) Finally, we have computed the long-time self-diffusion coefficient as defined in the fluid state through

$$D_L = \lim_{t \rightarrow \infty} \left[\left\langle \frac{1}{N} \sum_{i=1}^N (\vec{r}_i(t) - \vec{r}_i(0))^2 \right\rangle / 6t \right]. \quad (11)$$

The long-time limit can be estimated in a computer simulation by an extrapolation method similar to that used for the equilibrium case [35–39]. One example of the temperature

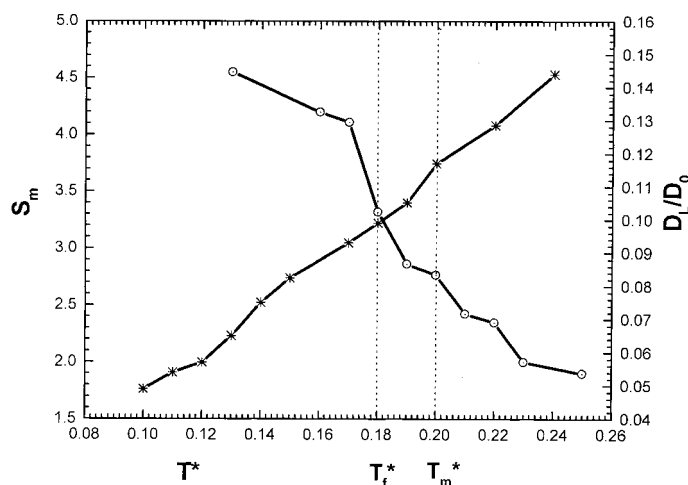


Figure 3. Height S_m of the maximal structure factor peak (circles, left y-axis) and the ratio D_L/D_0 (stars, right y-axis) versus reduced temperature T^* during a cooling process. The estimates of the reduced freezing and melting temperatures T_f^* and T_m^* are indicated by the vertical dashed lines. The parameters are as for figure 1.

dependence of D_L/D_0 is shown in figure 3, revealing that D_L/D_0 decreases significantly upon decreasing the temperature. Further results are summarized in table 1 together with the uncertainties caused by T_0^* .

As can indeed be concluded from table 1, the freezing and melting criteria are stable with respect to a non-equilibrium situation. L stays at around 0.18, well in the range relevant for equilibrium melting of Yukawa systems [7], and is pretty robust upon a change in field frequency and polydispersity. The maximum S_m of the first peak in the fluid structure factor also falls into an interval between 2.7 and 3.4; thereby, the Hansen–Verlet rule is stable with respect to non-equilibrium situations. The main cause for the deviation of S_m is the error in determining the phase transition temperature. Finally, the ratio D_L/D_0 of long-time to short-time diffusion is indeed about 10%, implying that the LPS rule is valid in non-equilibrium. We finally note that among the parameter combinations shown in table 1 there are also three equilibrium situations (i.e. $\omega \equiv 0$) of binary and polydisperse systems. Hence, as a by-product, our results also confirm the validity of the melting/freezing rules in equilibrium for binary or polydisperse systems. However, for stronger polydispersities, the system does not recrystallize but freezes into an amorphous glass [34] for a continuous charge distribution or exhibits lane formation of equally charged particles for a bimodal charge distribution [24, 40]. Since a non-equilibrium freezing transition is lost under these circumstances, a systematic study of these situations has not been pursued further here but will be published elsewhere.

In order to understand in more detail why the Lindemann criterion still holds, we have further explored the *anisotropy* of the mean square involved in its definition (8). For other anisotropic equilibrium systems, such as interacting particles in one-dimensional periodic grooves, it is known that the anisotropy of particle displacements may trigger unusual phenomena such as re-entrant melting [41–45] which violates the Lindemann rule (so-called laser-induced melting [24]). The same is true for freezing of circular rings in two-dimensional confined systems [46, 47]. In our case, as the external electric field sets a preferred direction, the particle displacements are inherently anisotropic. In order to quantify the anisotropy, we

define a dimensionless anisotropy parameter α as

$$\alpha = 2 \left\langle \frac{1}{N} \sum_{i=1}^N (z_i(t) - \langle z_i(t) \rangle)^2 \right\rangle / \left\langle \frac{1}{N} \sum_{i=1}^N [(x_i(t) - \langle x_i(t) \rangle)^2 + (y_i(t) - \langle y_i(t) \rangle)^2] \right\rangle. \quad (12)$$

In the monodisperse or field-free isotropic cases, α is evidently equal to 1, whereas, for a polydisperse sample, the shaking electric field will lead to larger distortion in the z -direction relative to the x - and y -directions, so we expect $\alpha > 1$. A typical example of the anisotropy parameter versus temperature is shown in figure 4. Two facts can be concluded from this figure. First, α is decreasing with temperature. This could be expected, as temperature increases the displacements equally in all three directions and thus reduces the anisotropy. Second, although α is definitively different from unity, the deviations are not large. In particular, near the melting point, $\alpha \approx 1.1$ which implies that the anisotropy is still small. This explains why the Lindemann rule is still applicable. If α had been much larger than 1, the system would consist of driven rows where—in analogy to laser-induced melting—the physics of the melting process is qualitatively different. As a final remark, we state that the long-time diffusion is also anisotropic in the fluid phase [48]; its relative anisotropy is small and comparable to α near the transition, explaining why the LPS criterion is still applicable.

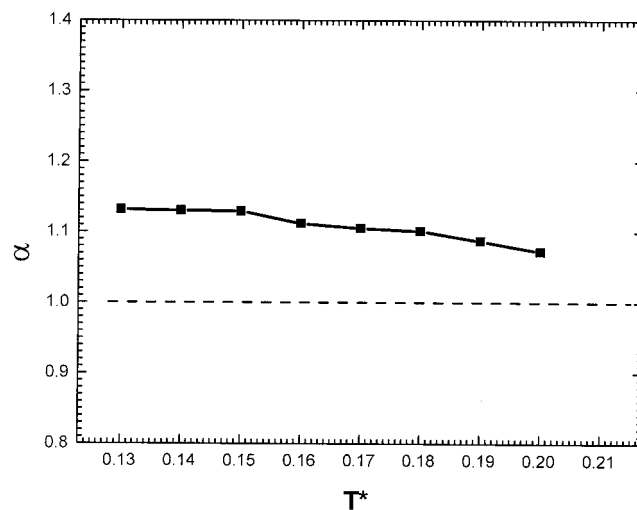


Figure 4. Anisotropy parameter α in the crystalline phase versus temperatures T^* for $p_Z = 0.15$ (■) and $\omega\tau = 6.28$. For comparison, the equilibrium result $\alpha \equiv 1$ is indicated as a dashed horizontal line.

5. Conclusions

In conclusion, we have confirmed the validity of various empirical freezing and melting criteria in steady-state non-equilibrium situations, induced by a shaking electric field acting on charge-polydisperse colloidal particles. The deviation from equilibrium can be controlled in our model by the relative polydispersity. We have shown that the criteria are valid provided the polydispersity is not too large, such that crystallization is not pre-empted by glass or lane formation. When field-induced crystallization occurred, the fluctuations were still almost isotropic, in clear distinction to highly anisotropic systems, which exhibit a different physics of melting. The criteria are surprisingly stable and this gives confidence

in the expectation that they also hold in different situations of a non-equilibrium steady state, e.g., oscillatory shear flow [49–52]. It would be interesting to establish the validity of these criteria within a more microscopical theoretical picture. This requires, however, a generalization of the current equilibrium approaches [17] to non-equilibrium situations. Another important research direction should incorporate the hydrodynamic interactions. While these are irrelevant for L and S_m in equilibrium, they play a crucial role for dynamical equilibrium correlations and control the non-equilibrium for concentrated suspensions. The inclusion of hydrodynamic interactions in driven systems may lead to further interesting phenomena, such as electrohydrodynamically induced pattern formation [53, 54]. Finally, a direct experimental verification of the freezing criteria should be carried out. One advantage of experiments is that the location of the non-equilibrium phase transition can be determined more precisely than in the computer simulation.

Acknowledgments

We thank J Dzubiella, C N Likos and T Palberg for helpful comments.

References

- [1] Baus M, Rull L F and Ryckaert J P (ed) 1995 *Physics (Observation, Prediction and Simulation of Phase Transitions in Complex Fluids Series B)* (Dordrecht: Kluwer Academic)
- [2] Singh Y 1991 *Phys. Rep.* **201** 351
- [3] Löwen H 1994 *Phys. Rep.* **237** 249
- [4] Lindemann F A 1910 *Phys. Z.* **11** 609
- [5] Ubbelohde A R 1978 *The Molten State of Matter* (Chichester: Wiley)
- [6] Lawson A C 2001 *Phil. Mag.* **B 81** 255
- [7] Meijer E J and Frenkel D 1991 *J. Chem. Phys.* **94** 2269
- [8] Löwen H, Palberg T and Simon R 1993 *Phys. Rev. Lett.* **70** 1557
- [9] Fröhlich J and Pfister C 1981 *Commun. Math. Phys.* **81** 277
- [10] Zahn K and Maret G 2000 *Phys. Rev. Lett.* **85** 3656
- [11] Finken R, Schmidt M and Löwen H 2001 *Phys. Rev. E* at press
- [12] Lang A, Likos C N, Watzlawek M and Löwen H 2000 *J. Phys.: Condens. Matter* **12** 5087
- [13] Heni M and Löwen H 2001 *J. Phys.: Condens. Matter* **13** 4675
- [14] Hansen J-P and Verlet L 1969 *Phys. Rev.* **184** 151
- [15] Broughton J Q, Gilmer G H and Weeks J D 1982 *Phys. Rev. B* **25** 4651
- [16] Löwen H 1996 *Phys. Rev. E* **53** R29
- [17] Banchio A J, Nägele G and Bergenholtz J 2000 *J. Chem. Phys.* **113** 3381
- [18] Pesche R, Kollmann M and Nägele G 2001 *J. Chem. Phys.* **114** 8701
- [19] Palberg T 1999 *J. Phys.: Condens. Matter* **11** R323
- [20] A further criterion, based on the vanishing residual multi-particle entropy, was put forward by Giaquinta *et al.*: Giaquinta P V, Giunta G and Giarritta S P 1992 *Phys. Rev. A* **45** R6966 but it has no immediate generalization to non-equilibrium systems.
- [21] Schmitz R 1994 *Physica A* **206** 25
- [22] Frink L J D, Thompson A and Salinger A G 2000 *J. Chem. Phys.* **112** 7564
- [23] For a review on driven diffusive systems, see Schmittmann B and Zia R K P 1995 *Phase Transitions and Critical Phenomena* vol 17, ed C Domb and J L Lebowitz (London: Academic)
- [24] Löwen H 2001 *J. Phys.: Condens. Matter* **13** R415
- [25] Grier D G and Murray C A 1994 *J. Chem. Phys.* **100** 9088
- [26] Löwen H and Hoffmann G 1999 *Phys. Rev. E* **60** 3009
- [27] Tata B V R and Arora A K 1991 *J. Phys.: Condens. Matter* **3** 7983
- [28] For a review, see Tata B V R and Arora A K 1996 *Ordering and Phase Transitions in Charged Colloids (VCH Series of Textbooks on Complex Fluids and Fluid Microstructures)* ed A K Arora and B V R Tata (New York: VCH) pp 181–206

- [29] Löwen H, Roux J N and Hansen J-P 1991 *Phys. Rev. A* **44** 1169
Löwen H, Hansen J-P and Roux J N 1991 *J. Phys.: Condens. Matter* **3** 997
- [30] D'Aguanno B and Klein R 1991 *J. Chem. Soc. Faraday Trans.* **87** 379
D'Aguanno B and Klein R 1992 *Phys. Rev. A* **46** 7652
- [31] Ermak D L 1975 *J. Chem. Phys.* **62** 4189
Ermak D L 1975 **62** 4197
- [32] Steinhardt P J, Nelson D R and Ronchetti M 1983 *Phys. Rev. B* **28** 784
- [33] van Duijneveldt J S and Frenkel D 1992 *J. Chem. Phys.* **96** 4655
- [34] More results and details can be found in
Hoffmann G P 2001 Phase transitions of colloidal suspensions in equilibrium and non-equilibrium *PhD Thesis*
Heinrich-Heine-Universität Düsseldorf
- [35] Löwen H and Szamel G 1993 *J. Phys.: Condens. Matter* **5** 2295
- [36] Bitzer F, Palberg T, Löwen H, Simon R and Leiderer P 1994 *Phys. Rev. E* **50** 2821
- [37] Heyes D M and Branka A C 1994 *Phys. Rev. E* **50** 2377
- [38] Rastogi S R, Wagner N J and Lustig S R 1996 *J. Chem. Phys.* **104** 9234
- [39] Bergenholtz J and Wagner N J 1997 *Physica A* **235** 34
- [40] Dzubiella J, Hoffmann G P and Löwen H 2001 Lane formation in binary colloidal suspensions driven by an external field *Phys. Rev. E* at press
- [41] Chakrabarti J, Krishnamurthy H R and Sood A K 1994 *Phys. Rev. Lett.* **73** 2923
- [42] Chakrabarti J, Krishnamurthy H R, Sood A K and Sengupta S 1995 *Phys. Rev. Lett.* **75** 2232
- [43] Wei Q H, Bechinger C, Rudhardt D and Leiderer P 1998 *Phys. Rev. Lett.* **81** 2606
- [44] Radzihovsky L, Frey E and Nelson D R 2001 *Phys. Rev. E* **63** 031503
- [45] For a review, see
Bechinger C and Frey E 2001 *J. Phys.: Condens. Matter* **13** R321
- [46] Bubeck R, Bechinger C, Nesper S and Leiderer P 1999 *Phys. Rev. Lett.* **82** 3364
- [47] Schweigert I V, Schweigert V A and Peeters F M 2000 *Phys. Rev. Lett.* **86** 4711
- [48] For a related phenomenon, namely anisotropy of long-time self-diffusion in the nematic phase, see:
Löwen H 1999 *Phys. Rev. E* **59** 1989
- [49] Heyes D M and Mitchell P J 1994 *J. Chem. Soc. Faraday Trans.* **90** 1931
- [50] Haw M D, Poon W C K, Pusey P N, Hebraud P and Lequeux F 1998 *Phys. Rev. E* **58** 4673
- [51] Dhont J K G and Nägele G 1998 *Phys. Rev. E* **58** 7710
- [52] Komatsugawa H and Nosé S 2000 *J. Chem. Phys.* **112** 11 058
- [53] Hu Y, Glass J L, Griffith A E and Fraden S 1994 *J. Chem. Phys.* **100** 4674
- [54] Isambert H, Ajdari A, Viovy J-L and Prost J 1997 *Phys. Rev. E* **56** 5688